ESC European Society of Cardiology

European Heart Journal - Cardiovascular Imaging (2023) **00**, 1–10
https://doi.org/10.1093/ehjci/jead319

ORIGINAL PAPER

Assessment of myocardial injuries in ischaemic and non-ischaemic cardiomyopathies using magnetic resonance T1-rho mapping

Aurélien Bustin [1,2,3]*, Xavier Pineau[2], Soumaya Sridi[2], Ruud B. van Heeswijk[3], Pierre Jaïs[1,4], Matthias Stuber[1,3,5], and Hubert Cochet[1,2]

[1]IHU LIRYC, Electrophysiology and Heart Modeling Institute, Université de Bordeaux, INSERM, Centre de recherche Cardio-Thoracique de Bordeaux, U1045, Avenue du Haut Lévêque, 33604 Pessac, France; [2]Department of Cardiovascular Imaging, Hôpital Cardiologique du Haut-Lévêque, CHU de Bordeaux, Avenue de Magellan, 33604 Pessac, France; [3]Department of Diagnostic and Interventional Radiology, Lausanne University Hospital and University of Lausanne, Rue du Bugnon 46, 1011 Lausanne, Switzerland; [4]Department of Cardiac Electrophysiology, Hôpital Cardiologique du Haut-Lévêque, CHU de Bordeaux, Avenue de Magellan, 33604 Pessac, France; and [5]Center for Biomedical Imaging (CIBM), Rue du Bugnon 46, 1011 Lausanne, Switzerland

Received 18 June 2023; revised 30 October 2023; accepted 16 November 2023; online publish-ahead-of-print 21 November 2023

Aims

To identify clinical correlates of myocardial T1ρ and to examine how myocardial T1ρ values change under various clinical scenarios.

Methods and results

A total of 66 patients (26% female, median age 57 years [Q1–Q3, 44–65 years]) with known structural heart disease and 44 controls (50% female, median age 47 years [28–57 years]) underwent cardiac magnetic resonance imaging at 1.5 T, including T1ρ mapping, T2 mapping, native T1 mapping, late gadolinium enhancement, and extracellular volume (ECV) imaging. In controls, T1ρ positively related with T2 ($P = 0.038$) and increased from basal to apical levels ($P < 0.001$). As compared with controls and remote myocardium, T1ρ significantly increased in all patients' sub-groups and all types of myocardial injuries: acute and chronic injuries, focal and diffuse tissue abnormalities, as well as ischaemic and non-ischaemic aetiologies ($P < 0.05$). T1ρ was independently associated with T2 in patients with acute injuries ($P = 0.004$) and with native T1 and ECV in patients with chronic injuries ($P < 0.05$). Myocardial T1ρ mapping demonstrated good intra- and inter-observer reproducibility (intraclass correlation coefficient = 0.86 and 0.83, respectively).

Conclusion

Myocardial T1ρ mapping appears to be reproducible and equally sensitive to acute and chronic myocardial injuries, whether of ischaemic or non-ischaemic origins. It may thus be a contrast-agent-free biomarker for gaining new and quantitative insight into myocardial structural disorders. These findings highlight the need for further studies through prospective and randomized trials.

*Corresponding author. E-mail: aurelien.bustin@ihu-liryc.fr

Graphical Abstract

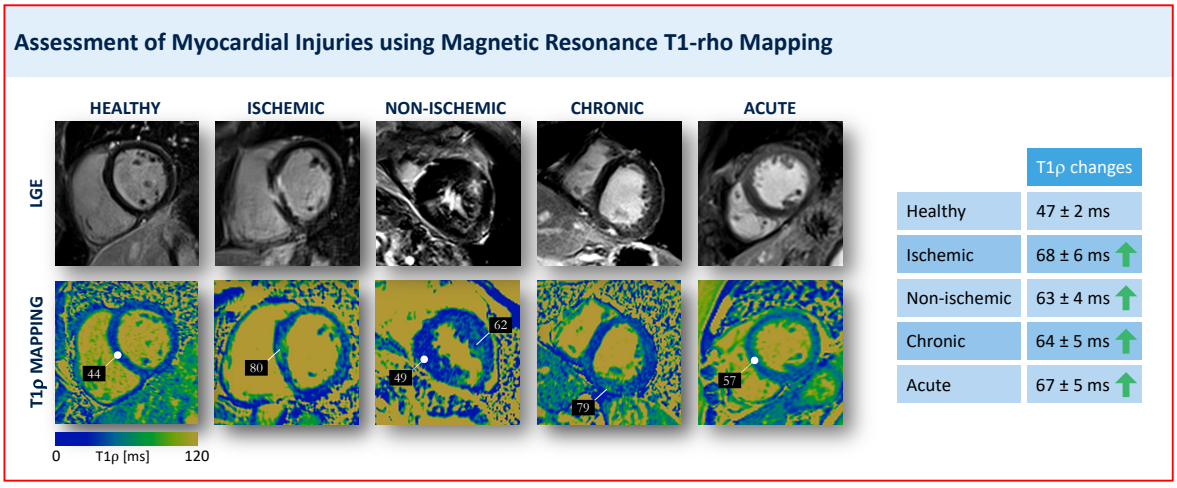

Keywords T1-rho • cardiomyopathy • myocardial scar • cardiovascular magnetic resonance

Introduction

Late gadolinium enhancement (LGE) cardiovascular magnetic resonance (CMR) imaging is the cornerstone technique to assess myocardial necrosis and focal replacement fibrosis.[1,2] However, the LGE method cannot distinguish between acute and chronic injuries, and its sensitivity to diffuse tissue changes remains limited by the need for a healthy myocardial reference. To overcome these issues, parametric mapping techniques such as T1 and T2 mapping have been successfully introduced. Combining LGE with multi-parametric mapping has greatly improved our understanding of cardiac diseases and is currently recommended for the diagnosis and prognosis of structural heart diseases.[3,4] However, as this approach requires multiple pre- and post-contrast scans, it is associated with prolonged scan times with significant impact on healthcare costs and CMR availability. In addition, the need for gadolinium-based contrast agents is increasingly being viewed as a clinical issue.[5,6] Therefore, a single non-contrast CMR technique that could accurately and quantitatively detect myocardial injuries would be immensely valuable. Myocardial T1-rho (T1ρ) mapping has emerged as a promising CMR tool to characterize the myocardium without injection of contrast agent. T1ρ relaxation occurs when transverse magnetization is spin-locked (i.e. no phase dispersion occurs) through the application of a continuous low-power radiofrequency pulse.[7–9] So far, *in vivo* applications of T1ρ mapping have been limited to a few studies reporting elevated T1ρ values in patients with myocardial infarction,[10–13] hypertrophic,[14,15] and dilated cardiomyopathies,[16] and in patients with end-stage renal disease.[17] Yet, the tissue determinants driving T1ρ changes remain unclear, and the applicability of the technique to the broad spectrum of acute and chronic myocardial injuries encountered in the clinic remains uncharted territory. In this exploratory study, we sought to (i) identify clinical correlates of myocardial T1ρ and (ii) examine how myocardial T1ρ values change under various clinical scenarios.

Methods

Population and study design

From October 2020 to December 2020, 69 patients undergoing CMR in our institution were prospectively included. The inclusion criterion was a clinical indication to undergo contrast-enhanced CMR as part of standard care. Non-inclusion criteria included age < 18 years old, history of allergic reaction to gadolinium-based contrast agents, history of severe renal failure, presence of a non-MR-conditional implantable device, inability to lay on the back for 50 min, pregnancy, breast-feeding, and inability to express informed consent. Patients were not consecutive as the inclusion depended on the clinical workflow and was also impacted by competing research projects on similar patients. In this patient population, T1ρ changes were analysed in relation to patient clinical history and other CMR findings. Over the same period, a cohort of 44 healthy volunteers was also prospectively recruited through advertising in the hospital. These individuals were originally recruited to form a control group in a separate project related to COVID-19 (ClinicalTrials.gov identifier: NCT04636320). This control population was used to define normal T1, T2, and T1ρ values and to analyse demographics correlates. The study was approved by our Institutional Ethics Committee, and all patients and volunteers provided informed consent.

Cardiac magnetic resonance protocol

All patients underwent standard CMR in the supine position on a 1.5 T clinical scanner (MAGNETOM Aera, Siemens Healthcare) with a 32-channel spine coil and a dedicated 18-channel body coil. The CMR protocol (see Supplementary data online, *Figure S1*) included a standard cine balanced steady-state free-precession (bSSFP) imaging in two-, three-, and four-chamber views, and in a stack of contiguous short-axis slices encompassing the ventricles. T2 mapping was performed using a T2-prepared bSSFP sequence[18] in a stack of continuous 8 mm thick short-axis slices covering the whole left ventricle.

Myocardial T1ρ maps were acquired pre-contrast using a breath-held bSSFP sequence incorporating an adiabatic T1ρ preparation module to achieve T1ρ-weighting.[19] Five T1ρ-weighted images with different spin lock times (TSL = [0, 10, 20, 35, 50] ms) were acquired sequentially in mid-diastole during 13 heartbeats (with a repetition time of 3 heartbeats to allow for full magnetization recovery). Three short-axis slices were acquired (basal, medial, and apical) for each patient. The T1ρ mapping sequence is illustrated in *Figure 1* and is described in detail in Bustin *et al.*[20]

Breath-held T1 mapping was performed at the same slice positions than T2 and T1ρ mapping using a modified Look-Locker inversion recovery

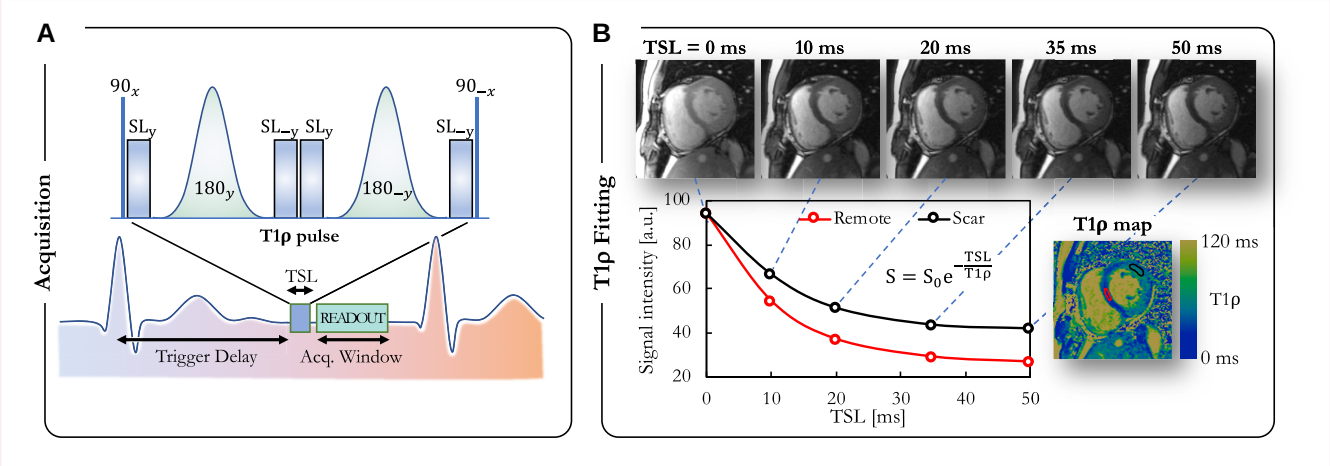

Figure 1 Myocardial T1ρ mapping framework. (*A*) Schematic of the 2D myocardial T1ρ mapping technique. T1ρ mapping is performed using a single-shot electrocardiogram-triggered balanced steady-state free-precession sequence. (*B*) Five single-shot T1ρ-weighted images are acquired at different spin lock times (TSL) along the T1ρ decay curve. A T1ρ map is generated inline using a model-based non-rigid motion-corrected reconstruction. The curves shown in (*B*) are from acquired data.

(MOLLI) sequence[21] with a 5(3)3 scheme before and 12 min after the administration of 0.2 mmol/kg gadoteric meglumine (Dotarem, Guerbet, France). Extracellular volume (ECV) was computed as in Flett *et al.*[22] using a haematocrit measurement performed on the day of the CMR study. LGE imaging was performed 15 min post-contrast using a breath-held phase-sensitive inversion recovery (PSIR) sequence[23] in a short-axis stack of contiguous slices encompassing the ventricles. Inversion times were adjusted to null viable myocardium. Typical parameters for the CMR sequences are outlined in Supplementary data online, *Table S1*.

Data analysis

All CMR images and maps were analysed by a radiologist (H.C., >15 years of CMR experience) using a commercially available software (CVI42, Circle Cardiovascular Imaging, Calgary, Canada). Matching two-dimensional short-axis slices were compared across T2 mapping, T1ρ mapping, native T1 mapping, ECV mapping, and LGE imaging. Left ventricular (LV) and right ventricular volumes, LV mass, LVEF, and wall motion abnormalities were analysed from end-diastolic and end-systolic short-axis cine views according to current guidelines.[24] Mass and volumes were indexed to body surface area. Maximum LV wall thickness was measured on cine short-axis images at end-diastole. Focal injuries were identified by PSIR-LGE and reported on the 16-segment American Heart Association (AHA) model.[25] The distribution of LGE was categorized as subendocardial, subepicardial, and/or mid-wall. LGE was considered transmural if involving the entire myocardial thickness on at least one location. Endocardial and epicardial contours were traced on T1, T2, T1ρ, and ECV maps by avoiding contamination by LV blood signal and extra-myocardial structures. Mean myocardial relaxation times were extracted from the 16 LV segments of the AHA model. Furthermore, mean T1, T2, T1ρ, and ECV values were measured in both the remote (mid-ventricular slice) and injured myocardium by drawing regions of interest (ROIs) over the maps. Injured and remote areas were defined as regions with and without LGE, respectively. The size of the ROIs in remote regions was ≥65 pixels whereas the size of the ROIs in injured regions was dictated by the LGE boundaries (ranging from 74 to 2000 mm^2). In controls, the remote ROI was measured in the septal region of the medial short-axis slice. The T1ρ, T2, native T1, and ECV values in controls were used to establish cut-off thresholds that were set at 2 SD above the mean remote values. To test inter- and intra-observer reproducibility, injured and remote ROIs were drawn twice on all myocardial T1ρ maps by the same reader (within a 3-month interval to prevent recall bias) and by a second reader. The presence of artefacts caused by mistriggering, incorrect motion correction, and susceptibility artefacts was assessed by examination of the raw T1ρ-weighted images and corresponding T1ρ maps.

Clinical diagnosis

The aetiological diagnosis was determined based on clinical history, clinical symptoms, available non-CMR tests (biology, electrocardiography, echocardiography, computed tomography), and CMR findings. The criteria used to diagnose cardiac diseases are provided in Supplementary data online, *Methods*. Underlying diseases were categorized as either ischaemic or non-ischaemic. In addition, myocardial injuries were defined as either acute or chronic, acute injuries being defined by the presence of elevated myocardial T2 values.

Statistical analysis

Statistical analysis was performed using SPSS version 27 (IBM Corp., Armonk, New York). Results are presented using conventional descriptive statistics. The Shapiro–Wilk test was used to test the null hypothesis that each continuous variable follows a normal distribution. Continuous variables are presented as mean ± standard deviation and as median [interquartile range Q1–Q3] otherwise. Categorical variables are presented as fraction (%). Continuous variables were compared using parametric (unpaired Student's *t*-test) or non-parametric tests (Mann–Whitney), depending on data normality. Paired Student's *t*-tests were used for statistical comparison between remote and injured segments. Categorical variables were compared using the χ^2 test or the Fisher's exact test, as appropriate. Statistical significance differences between slices, AHA segments, and patient groups were determined using a one-way analysis of variance followed by Tukey's *post hoc* test for multiple comparison. In patients and controls, univariable analyses were performed using Pearson's correlation coefficient (*r*). To identify variables with independent association with T1ρ, a stepwise multivariable linear regression analysis was performed using the criterion of $P < 0.05$ on univariable analysis for inclusion in the multivariable model. Standardized regression coefficients (β) were reported. Inter- and intra-observer reproducibility were tested in all subjects by Bland–Altman analysis and intraclass correlation coefficient (ICC) with two-way mixed-effects model for absolute agreement. An ICC above 0.75 was an indicator of good reproducibility. All statistical tests were two-tailed, with *P*-values of <0.05 considered to indicate statistical significance.

Table 1 Characteristics of study subjects ($n = 110$)

	Patients ($n = 66$)	Controls ($n = 44$)	*P*-value
Demographics			
Female gender	17 (26)	22 (50)	<0.001*
Age, years	57 [44–65]	47 [28–57]	0.003*
Weight, kg	77 ± 16	69 ± 12	0.005*
Height, cm	172 ± 9	170 ± 10	0.432
BMI, kg/m^2	26 ± 5	24 ± 3	0.005*
Risk factors			
Hypertension	11 (17)	2 (5)	0.064
Dyslipidaemia	8 (12)	0 (0)	<0.001*
Diabetes mellitus	4 (6)	1 (2)	0.374
Smoking	23 (35)	4 (9)	0.003*
Obesity (BMI ≥ 30 kg/m^2)	13 (20)	1 (2)	0.009*
Family history of coronary artery disease	12 (18)	0 (0)	<0.001*
Pre-CMR findings			
Resting heart rate, beats/min	66 [59–76]	63 [57–68]	0.218
Systolic blood pressure, mmHg	128 [110–133]	135 [122–146]	0.008*
Diastolic blood pressure, mmHg	73 [66–80]	82 [69–96]	0.007*
NT-proBNP, pg/mL	350 [37–1137]	69 [54–83]	0.005*
AF/atrial flutter	3 (5)	1 (2)	0.561
Haematocrit, %	41 ± 6	42 ± 3	0.817
CMR function			
LVEDV$_i$, mL/m^2	101 ± 32	85 ± 16	0.006*
LVESV$_i$, mL/m^2	53 ± 31	35 ± 9	<0.001*
LVEF, %	48 ± 14	58 ± 6	<0.001*
LV mass, g/m^2	59 [52–69]	53 [47–63]	0.827
LV wall motion abnormality	41 (62)	0 (0)	<0.001*
LV maximum thickness, mm	10.5 ± 2.2	8.7 ± 2.0	<0.001*
RVEDV$_i$, mL/m^2	83 ± 24	83 ± 13	0.938
RVESV$_i$, mL/m^2	41 ± 17	39 ± 10	0.462
RVEF, %	50 ± 11	55 ± 7	0.075
CMR tissue characterization			
LV T1ρ, ms	48 ± 4	47 ± 2	0.029*
Elevated T1ρ (≥51 ms)	49 (74)	NA	NA
LV T2, ms	49 ± 6	46 ± 3	0.006*
Elevated T2 (≥51 ms)	36 (55)	NA	NA
LV native T1, ms	1035 ± 55	1010 ± 23	0.036*
Elevated native T1 (≥1057 ms)	37 (56)	NA	NA
LV ECV, %	27 ± 6	25 ± 2	0.021*
Elevated ECV (≥29%)	40 (61)	NA	NA
Presence of LGE	45 (68)	0 (0)	<0.001*

Values are *n* (%), mean ± SD, or median [interquartile range].
AF, atrial fibrillation; BMI, body mass index; CMR, cardiac magnetic resonance; ECV, extracellular volume; LV, left ventricle; LVEDV$_i$, indexed left ventricular end-diastolic volume; LVESV$_i$, indexed left ventricular end-systolic volume; LVEF, left ventricular ejection fraction; NA, not applicable; RVEDV$_i$, right ventricular end-diastolic volume; RVESV$_i$, right ventricular end-systolic volume; RVEF, right ventricular ejection fraction.
*$P < 0.05$ between patients and controls.

Table 2 Post-CMR diagnoses in the patient cohort ($n = 66$)

	Total	Acute	Chronic
Ischaemic heart disease	18 (27)	6 (9)[a]	13 (20)[a]
Non-ischaemic heart disease	48 (73)	8 (12)	40 (61)
Dilated cardiomyopathy	22 (33)	0 (0)	22 (33)
Hypertrophic cardiomyopathy	7 (11)	1 (2)	6 (9)
Myocarditis	9 (14)	3 (5)	6 (9)
Takotsubo cardiomyopathy	4 (6)	3 (5)	1 (2)
Arrhythmogenic cardiomyopathy	2 (3)	0 (0)	2 (3)
Amyloidosis	1 (2)	0 (0)	1 (2)
Cardiac sarcoid	1 (2)	1 (2)	0 (0)
Eosinophilic granulomatosis with polyangiitis	2 (3)	0 (0)	2 (3)

Values are expressed as number (%).
[a]One patient counted twice because showing both chronic post-infarction scar and acute myocardial infarction in different vascular territories.

Results

Population

A flow diagram of patients' recruitment is shown in Supplementary data online, *Figure S2*. Of 69 patients enrolled, three were excluded (one due to inadequate image quality and two due to claustrophobia before CMR). The studied population thus comprised a total of 66 patients (26% female, median age 57 years [Q1–Q3, 44–65 years]) and 44 healthy controls (50% female, median age 47 years [28–57 years]). The baseline characteristics of the studied population are reported in *Table 1*. Controls were younger ($P = 0.003$) and had lower body mass index (BMI, $P = 0.005$) than patients. No differences in heart rate were observed between the two cohorts ($P = 0.218$). LVEF by CMR was lower in patients than in controls (48 ± 14% vs. 58 ± 6%, $P < 0.001$). Final diagnoses in the patient population are detailed in *Table 2*. The aetiological diagnosis was ischaemic in 18 (27%) and non-ischaemic in 48 (73%). Acute myocardial injuries were found in 14 (21%) patients.

Myocardial T1ρ mapping in controls

The quality assessment of T1ρ maps and the reproducibility of T1ρ measurements are provided in Supplementary data online, *Results*. Bland–Altman suggested good intra-observer (ICC = 0.86)

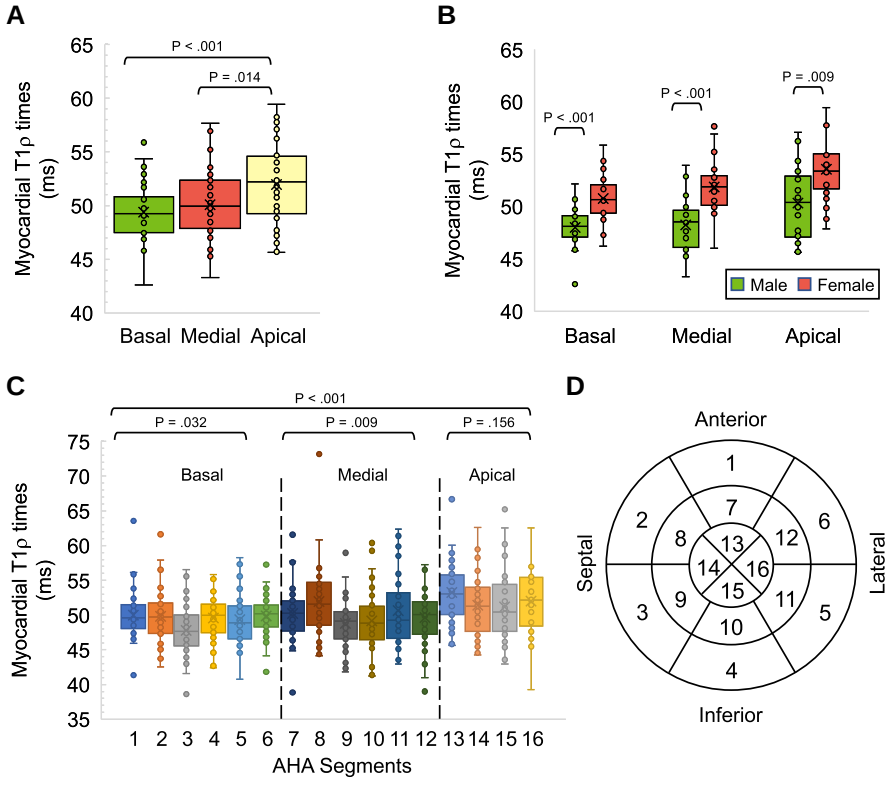

Figure 2 Regional variations of myocardial T1ρ values in controls. (*A*) Myocardial T1ρ variations on the basal, medial, and apical short-axis levels. (*B*) Myocardial T1ρ values according to gender. (*C*) Myocardial T1ρ values extracted from the 16 left ventricular segments of the American Heart Association model (*D*). The centre cross in each box denotes the mean, the centre line represents the median, and the lower and upper limits of each box represent the first and third quartiles, respectively. Outliers are displayed as individual dots.

Table 3 Multivariable analysis of parameters associated with septal myocardial T1ρ in controls ($n = 44$)

	Univariable analysis		Multivariable analysis	
	r	*P*-value	Standardized *β*	*P*-value
Demographics				
Age	0.437	0.003	0.301	0.074
Gender	0.414	0.005	−0.359	0.108
Weight	−0.309	0.041	0.109	0.623
Height	−0.369	0.014	0.009	0.976
Body mass index	−0.062	0.691	—	—
Resting heart rate	−0.141	0.361	—	—
CMR function				
$LVEDV_i$	0.244	0.110	—	—
$LVESV_i$	0.296	0.051	—	—
LVEF	0.225	0.142	—	—
LV mass	0.087	0.661	—	—
LV maximum thickness	0.165	0.359	—	—
$RVEDV_i$	0.358	0.086	—	—
$RVESV_i$	0.395	0.056	—	—
RVEF	0.241	0.256	—	—
CMR tissue characterization				
LV native T1	0.158	0.329	—	—
LV T2	0.616	<0.001	0.382	0.038
LV ECV	0.157	0.340	—	—

CMR, cardiac magnetic resonance; ECV, extracellular volume; $LVEDV_i$, indexed left ventricular end-diastolic volume; $LVESV_i$, indexed left ventricular end-systolic volume; LVEF, left ventricular ejection fraction; LV, left ventricle; $RVEDV_i$, right ventricular end-diastolic volume; $RVESV_i$, right ventricular end-systolic volume; RVEF, right ventricular ejection fraction.

and inter-observer (ICC = 0.83) reproducibility. In healthy volunteers, the mean septal T1ρ value was 47 ± 2 ms. There was a significant difference in T1ρ between slice locations and AHA segments ($P < 0.001$ for both, *Figure 2*). Global T1ρ values at the apical level (52 ± 4 ms) were higher than at median (50 ± 3 ms, $P = 0.014$) and basal levels (49 ± 3 ms,

Table 4 Multivariable analysis of parameters associated with myocardial T1ρ in patients ($n = 66$)

	Univariable analysis		Multivariable analysis	
	r	*P*-value	Standardized *β*	*P*-value
Ischaemic ($n = 18$)				
Native T1	0.432	0.095	—	—
T2	0.774	0.009	0.688	<0.001
ECV	0.586	0.028	0.567	0.002
Non-ischaemic ($n = 48$)				
Native T1	0.632	<0.001	0.078	0.078
T2	0.658	0.002	0.367	0.367
ECV	0.511	0.001	0.416	0.209
Acute ($n = 14$)				
Native T1	0.733	0.016	−0.271	0.386
T2	0.904	<0.001	1.438	0.004
ECV	0.776	0.008	−0.294	0.415
Chronic ($n = 53$)				
Native T1	0.530	<0.001	0.390	0.016
T2	0.412	0.071	—	—
ECV	0.562	<0.001	0.323	0.045

CMR, cardiac magnetic resonance; ECV, extracellular volume; $LVEDV_i$, indexed left ventricular end-diastolic volume; $LVESV_i$, indexed left ventricular end-systolic volume; LVEF, left ventricular ejection fraction; LV, left ventricle; $RVEDV_i$, right ventricular end-diastolic volume; $RVESV_i$, right ventricular end-systolic volume; RVEF, right ventricular ejection fraction.

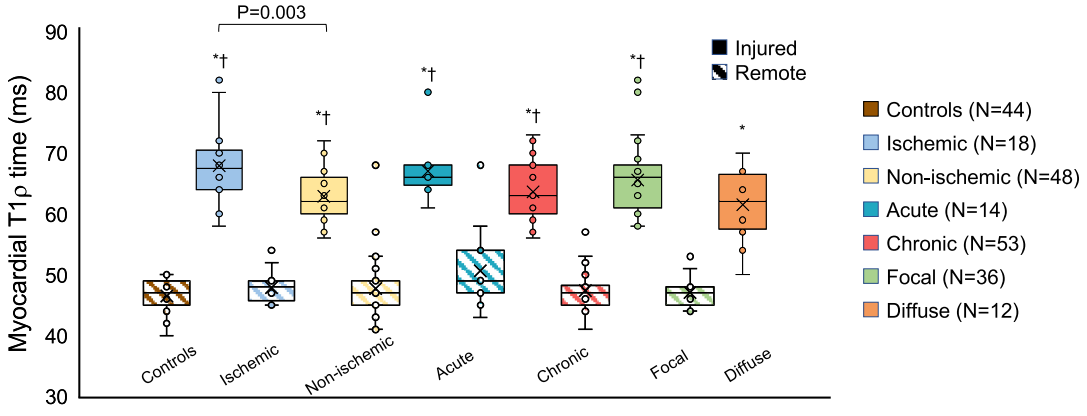

Figure 3 Averaged T1ρ values in the injured and remote segments in the different patient groups and in controls. Myocardial T1ρ values in patients were significantly higher in injured regions than in remote regions and in controls. *$P < 0.05$ for comparison to controls. †$P < 0.05$ for comparison to remote regions.

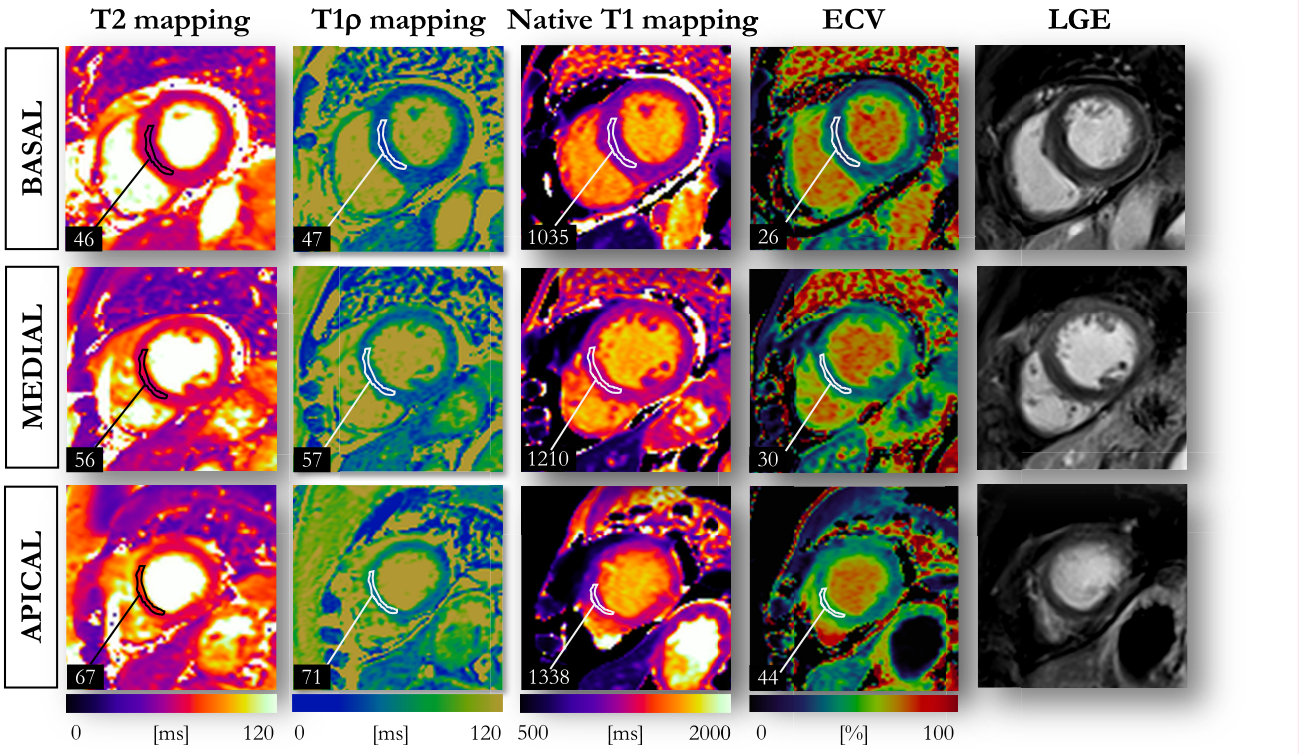

Figure 4 57-Year-old female patient with CMR findings consistent with Takotsubo cardiomyopathy. Myocardial T2 maps exhibit myocardial oedema at the medial and apical short-axis levels (T2 = 67 ms) with a clear T1ρ elevation at these locations (T1ρ = 71 ms) whereas LGE images show a lack of ischaemia and delayed hyper-enhancement.

$P < 0.001$). Septal T1ρ correlates are provided in *Table 3* and Supplementary data online, *Figure S3*. On univariable analysis, T1ρ positively related to T2 ($R = 0.62$, $P < 0.001$), age ($R = 0.44$, $P = 0.003$), and female gender ($R = 0.41$, $P = 0.005$), and inversely related to weight ($R = -0.31$, $P = 0.041$), and height ($R = -0.37$, $P = 0.014$). On multivariable analysis, T2 ($\beta = 0.38$, $P = 0.038$) was the only factor independently associated with T1ρ values. Measurements in healthy volunteers were used to define normal values on all myocardial parameters, the upper limit of normality being set to T1ρ = 51 ms, T2 = 51 ms, native T1 = 1057 ms, and ECV = 29%.

Myocardial T1ρ mapping in patients

Remote T1ρ value could be measured in 54/66 patients only, as 12 patients showed diffuse tissue abnormalities and therefore a lack of remote myocardium (seven patients with diffuse fibrosis, four with diffuse oedema, and one with diffuse amyloidosis). Mean remote T1ρ value in patients was 48 ± 4 ms ($P = 0.117$ vs. controls). *Figure 3* displays T1ρ values in injured vs. remote myocardium according to the underlying aetiology, the acute or chronic nature of the injury, and its focal or diffuse distribution. In each category, myocardial T1ρ values were significantly higher in injured regions without overlap with T1ρ values measured in remote myocardium. T1ρ correlates in patients are analysed in detail in *Table 4*, according to the underlying aetiology and to the acute or chronic nature of myocardial injuries.

T1ρ correlates in patients with acute and chronic myocardial injuries

In patients with acute myocardial injuries ($n = 14$), T2 was the only factor independently associated with T1ρ values ($\beta = 1.44$, $P = 0.004$). T2 and T1ρ values were both found to be elevated in all patients (T2 = 67 ± 8 ms, T1ρ = 67 ± 5 ms). Typical myocardial T1ρ maps in a patient with acute Takotsubo cardiomyopathy are shown in *Figure 4*.

In patients with chronic myocardial injuries ($n = 53$), native T1 ($\beta = 0.39$, $P = 0.016$) and ECV ($\beta = 0.32$, $P = 0.045$) were the two factors independently associated with T1ρ values. T1ρ relaxation times did not correlate with T2 ($R = 0.41$, $P = 0.071$). We found elevated native T1 (1143 ± 83 ms), ECV (44 ± 16%), and T1ρ (64 ± 5 ms) values in 52%, 59%, and 71% of patients, respectively.

T1ρ correlates in patients with ischaemic and non-ischaemic heart diseases

In patients with ischaemic heart disease ($n = 18$), T1ρ independently related to T2 ($\beta = 0.69$, $P < 0.001$) and ECV ($\beta = 0.57$, $P = 0.002$) on multivariable analysis. LGE was present in all patients. We found elevated T1ρ (68 ± 6 ms), native T1 (1213 ± 113 ms), and ECV (53 ± 17%) values in 18 (100%), 15 (83%), and 17 (94%) patients, respectively.

In patients with non-ischaemic heart diseases ($n = 48$), there was no factor independently associated with T1ρ values. LGE was present in 27 (56%) patients. We found elevated myocardial T1ρ (63 ± 4 ms), native T1 (1142 ± 76 ms), and ECV (37 ± 8%) values in 31 (65%), 22 (46%), and 23 (48%) patients, respectively. Representative examples of T1ρ maps alongside other CMR techniques from patients with ischaemic and non-ischaemic injuries are shown in *Figure 5*.

Discussion

This exploratory study provides the largest clinical experience to date on the use of myocardial T1ρ mapping in cardiac imaging

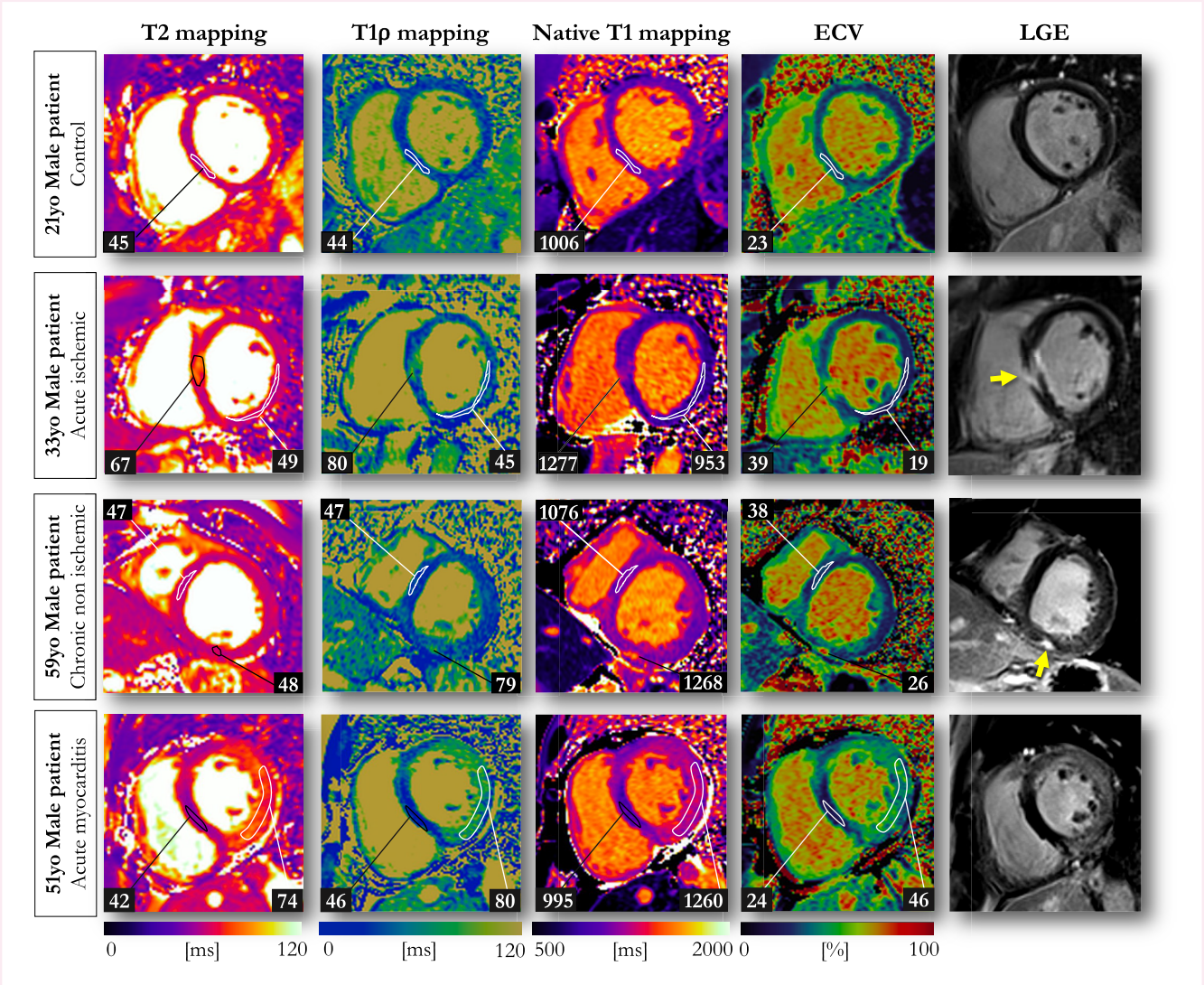

Figure 5 Examples of T1ρ maps in one control and three patients with heart disease. (*A*) 21-Year-old male patient (control) with normal T2 (45 ms), T1ρ (44 ms), native T1 (1006 ms), and normal LGE. (*B*) 33-Year-old male patient with acute ischaemic cardiomyopathy reflected by basal anteroseptal hyper-enhancements on LGE with T2 (67 ms) and T1ρ (80 ms) elevations. (*C*) 59-Year-old male patient with non-ischaemic dilated cardiomyopathy with subepicardial inferobasal hyper-enhancement on LGE with a clear T1ρ elevation in the same segment (79 ms) and normal T2 on T2 mapping (48 ms). (*D*) 51-Year-old male patient with acute myocarditis. Arrowheads indicate regions with myocardial injury.

(Central Illustration). Studying a series of patients with a wide spectrum of clinical presentations, with healthy volunteers for comparison, our main findings are that myocardial T1ρ:

(i) can be reproducibly measured in patients,
(ii) closely relates to T2 values and LGE in acute myocardial diseases,
(iii) closely relates to T1 values, ECV values, and LGE in chronic myocardial diseases, and
(iv) allows for a contrast-free detection of myocardial injuries irrespective of the underlying aetiology.

Normal myocardial T1ρ values and confounding factors

In this study, myocardial T1ρ values in controls were slightly lower than those reported in a previous study at 1.5 T (47 ± 2 ms vs. 52 ± 1 and 53 ± 2 ms).[12,16] This difference may be attributed to variations in T1ρ module, spin lock durations, and MR system used. It is important to note that these values were obtained with a spin lock frequency of 500 Hz, and are expected to differ for other frequencies and spin lock times. Our results in healthy volunteers also demonstrate a close relationship between T1ρ and T2, suggesting that T1ρ is a sensitive measure of water content, even in the absence of structural heart disease. We also found that myocardial T1ρ positively relates to age and female gender, which aligns with other myocardial tissue mapping techniques.[26,27] These findings are consistent with studies showing age-dependent collagen accumulation in the interstitial space, especially in males,[28,29] and the thinner myocardium in female subjects, which makes them more susceptible to partial volume effects. Further larger studies should establish age- and gender-specific normal ranges for myocardial T1ρ mapping. Lastly, normal T1ρ values were higher in apical segments, likely due to increased susceptibility to partial volume averaging, as previously reported for T2 and T1 mapping data.[27,30,31]

Myocardial T1ρ mapping: a promising non-contrast CMR marker?

The clinical significance of myocardial T1ρ mapping in patients with structural heart disease is incompletely understood. In this exploratory study, we sought to assess the potential of the technique across a broad spectrum of myocardial disorders reflecting the clinical scenarios encountered in a routine practice. Our results indicate that T1ρ mapping is equally sensitive to acute and chronic, as well as to ischaemic and non-ischaemic diseases. As compared with controls, we observed a T1ρ increase of 45% in ischaemic patients, 34% in non-ischaemic patients, 43% in chronic injuries, and 36% in acute injuries. Myocardial T1ρ prolongation in disease has also been described by other groups.[12,14,16,19] van Oorschot *et al.*[11] also observed a 46% increase in patients with chronic myocardial infarction. In the present study, we observed no overlap between the T1ρ values sampled in injured vs. remote areas in both the ischaemic and non-ischaemic populations, indicating that contrast-free T1ρ mapping can robustly and quantitatively characterize these tissues. In patients with acute myocardial injuries, T1ρ was positively correlated with T2. This phenomenon may be attributed to the occurrence of myocardial cell death following a myocardial infarction. Consequently, the dynamic interplay between water and macromolecules undergoes substantial alterations, resulting in a reduced impact of macromolecules on proton relaxation. This, in turn, leads to an extension of T1ρ values within the acutely infarcted myocardium.

We also found a significant association between myocardial T1ρ and ECV in patients with ischaemic and chronic injuries. Specifically, myocardial T1ρ mapping may hold potential in detecting concealed chronic myocardial injuries, particularly in the risk stratification of ventricular arrhythmias.

Our study demonstrated that, like T1, T1ρ is a relatively unspecific marker for myocardial disease. However, since T1ρ occurs at the frequency of slow tumbling macromolecules instead of the high MHz range, it should be more sensitive to changes in the concentration and behaviour of collagen fibres, and thus to interstitial fibrosis. In non-ischaemic heart disease, we found a lack of association between T1ρ and T1, T2, and ECV, which can be attributed to several significant factors, including the relatively small and heterogenous study cohort with a substantial proportion of negative exams. In acute heart disease, we observed a lack of correlation between T1ρ and pre-contrast T1 mapping and ECV, which raises important questions about the underlying mechanism of T1ρ elevation. Further studies in acute patient cohorts and in animals are required.

Finally, our results demonstrated a lack of specificity of the technique. This is likely to position myocardial T1ρ mapping as a valuable screening technique, without alleviating the need for other diagnostic techniques, including T2 mapping and post-contrast CMR, when T1ρ is positive.

Study limitations

The study has limitations. Firstly, the single-centre design of the study with relatively small sample size cannot exclude centre-specific T1ρ bias. Our established T1ρ ranges and thresholds at 1.5 T may be centre-, field strength-, and vendor-dependent. In our Supplementary data online, *Discussion*, we outline steps for achieving clinical acceptance and standardization of myocardial T1ρ mapping, with the potential for technology deployment in other clinical centres and multi-centric research. In this study, fibrotic extent and transmurality in ischaemic and non-ischaemic cardiomyopathies were not measured and compared against established LGE, native T1, T2, and ECV mapping techniques. This analysis has been delegated to future animal and human studies. Further investigation is now needed to assess the true sensitivity, specificity, diagnostic and prognostic value of T1ρ mapping in detecting acute and chronic myocardial injuries for specific clinical scenarios and underlying aetiologies.

In conclusion, non-contrast myocardial T1ρ mapping shows promise for the quantitative characterization of myocardial injuries. The technique appears to be equally sensitive to acute and chronic myocardial injuries, whether of ischaemic or non-ischaemic origins. Nevertheless, further studies through prospective, randomized trials are warranted to elucidate its clinical utility.

Supplementary data

Supplementary data are available at *European Heart Journal - Cardiovascular Imaging* online.

Funding

This research was supported by funding from the French National Research Agency under grant agreements Equipex MUSIC ANR-11-EQPX-0030, ANR-22-CPJ2-0009-01, ANR-21-CE17-0034-01, and Programme d'Investissements d'Avenir ANR-10-IAHU04-LIRYC, and from the European Research Council (ERC) under the European Union's Horizon 2020 research and innovation program (grant agreement N°101076351). A.B. acknowledges a Lefoulon-Delalande Foundation fellowship administered by the Institute of France.

Conflict of interest: None declared.

Data availability

As part of the Open Science and reproducible research initiative, we provide phantom and *in vivo* T1ρ-weighted datasets at this repository: https://github.com/AurelienBustin/T1-rho-mapping. This repository also contains fitting codes as well as the T1ρ colormap used in this article.

References

1. Kim RJ, Wu E, Rafael A, Chen E-L, Parker MA, Simonetti O *et al.* The use of contrast-enhanced magnetic resonance imaging to identify reversible myocardial dysfunction. *N Engl J Med* 2000;**343**:1445–53.
2. Kim RJ, Fieno DS, Parrish TB, Harris K, Chen E-L, Simonetti O *et al.* Relationship of MRI delayed contrast enhancement to irreversible injury, infarct age, and contractile function. *Circulation* 1999;**100**:1992–2002.
3. Almogheer B, Antonopoulos AS, Azzu A, Al Mohdar S, Vlachopoulos C, Pantazis A *et al.* Diagnostic and prognostic value of cardiovascular magnetic resonance in neuromuscular cardiomyopathies. *Pediatr Cardiol* 2022;**43**:27–38.
4. Leiner T, Bogaert J, Friedrich MG, Mohiaddin R, Muthurangu V, Myerson S *et al.* SCMR position paper (2020) on clinical indications for cardiovascular magnetic resonance. *J Cardiovasc Magn Reson* 2020;**22**:76.
5. Thomsen HS, Morcos SK, Almén T, Bellin M-F, Bertolotto M, Bongartz G *et al.* Nephrogenic systemic fibrosis and gadolinium-based contrast media: updated ESUR Contrast Medium Safety Committee guidelines. *Eur Radiol* 2013;**23**:307–18.
6. Guo BJ, Yang ZL, Zhang LJ. Gadolinium deposition in brain: current scientific evidence and future perspectives. *Front Mol Neurosci* 2018;**11**:335.
7. Han Y, Liimatainen T, Gorman RC, Witschey WR. Assessing myocardial disease using T1ρ MRI. *Curr Cardiovasc Imaging Rep* 2014;**7**:9248.
8. Michaeli S, Sorce DJ, Garwood M. T2ρ and T1ρ adiabatic relaxations and contrasts. *Curr Anal Chem* 2008;**4**:8–25.
9. Gilani IA, Sepponen R. Quantitative rotating frame relaxometry methods in MRI. *NMR Biomed* 2016;**29**:841–61.
10. Witschey WRT, Zsido GA, Koomalsingh K, Kondo N, Minakawa M, Shuto T *et al.* In vivo chronic myocardial infarction characterization by spin locked cardiovascular magnetic resonance. *J Cardiovasc Magn Reson* 2012;**14**:37.
11. van Oorschot JWM, El Aidi H, Jansen of Lorkeers SJ, Gho JM, Froeling M, Visser F *et al.* Endogenous assessment of chronic myocardial infarction with T1ρ-mapping in patients. *J Cardiovasc Magn Reson* 2014;**16**:104.
12. Van Oorschot JWM, Visser F, Eikendal ALM, Vonken EPA, Luijten PR, Chamuleau SAJ *et al.* Single breath-hold T1ρ-mapping of the heart for endogenous assessment of myocardial fibrosis. *Invest Radiol* 2016;**51**:505–12.
13. Stoffers RH, Madden M, Shahid M, Contijoch F, Solomon J, Pilla JJ *et al.* Assessment of myocardial injury after reperfused infarction by T1ρ cardiovascular magnetic resonance. *J Cardiovasc Magn Reson* 2017;**19**:17.
14. Wang C, Zheng J, Sun J, Wang Y, Xia R, Yin Q *et al.* Endogenous contrast T1rho cardiac magnetic resonance for myocardial fibrosis in hypertrophic cardiomyopathy patients. *J Cardiol* 2015;**66**:520–6.

15. Thompson EW, Kamesh Iyer S, Solomon MP, Li Z, Zhang Q, Piechnik S *et al.* Endogenous T1ρ cardiovascular magnetic resonance in hypertrophic cardiomyopathy. *J Cardiovasc Magn Reson* 2021;**23**:120.
16. van Oorschot JWM, Güçlü F, de Jong S, Chamuleau SAJ, Luijten PR, Leiner T *et al.* Endogenous assessment of diffuse myocardial fibrosis in patients with T1ρ-mapping. *J Magn Reson Imaging* 2017;**45**:132–8.
17. Wang L, Yuan J, Zhang SJ, Gao M, Wang Y-C, Wang Y-X *et al.* Myocardial T1rho mapping of patients with end-stage renal disease and its comparison with T1 mapping and T2 mapping: a feasibility and reproducibility study. *J Magn Reson Imaging* 2016;**44**: 723–31.
18. Giri S, Chung YC, Merchant A, Mihai G, Rajagopalan S, Raman SV *et al.* T2 quantification for improved detection of myocardial edema. *J Cardiovasc Magn Reson* 2009; **11**:56.
19. Qi H, Bustin A, Kuestner T, Hajhosseiny R, Cruz G, Kunze K *et al.* Respiratory motion-compensated high-resolution 3D whole-heart T1ρ mapping. *J Cardiovasc Magn Reson* 2020;**22**:12.
20. Bustin A, Toupin S, Sridi S, Yerly J, Bernus O, Labrousse L *et al.* Endogenous assessment of myocardial injury with single-shot model-based non-rigid motion-corrected T1 rho mapping. *J Cardiovasc Magn Reson* 2021;**23**:119.
21. Messroghli DR, Radjenovic A, Kozerke S, Higgins DM, Sivananthan MU, Ridgway JP. Modified Look-Locker inversion recovery (MOLLI) for high-resolution T1 mapping of the heart. *Magn Reson Med* 2004;**52**:141–6.
22. Flett AS, Hayward MP, Ashworth MT, Hansen MS, Taylor AM, Elliott PM *et al.* Equilibrium contrast cardiovascular magnetic resonance for the measurement of diffuse myocardial fibrosis: preliminary validation in humans. *Circulation* 2010;**122**: 138–44.
23. Kellman P, Arai AE, McVeigh ER, Aletras AH. Phase-sensitive inversion recovery for detecting myocardial infarction using gadolinium-delayed hyperenhancement. *Magn Reson Med* 2002;**47**:372–83.
24. Kramer CM, Barkhausen J, Bucciarelli-Ducci C, Flamm SD, Kim RJ, Nagel E. Standardized cardiovascular magnetic resonance imaging (CMR) protocols: 2020 update. *J Cardiovasc Magn Reson* 2020;**22**:17.
25. Cerqueira MD, Weissman NJ, Dilsizian V, Jacobs AK, Kaul S, Laskey WK *et al.* Standardized myocardial segmentation and nomenclature for tomographic imaging of the heart: a statement for healthcare professionals from the cardiac imaging. *Circulation* 2002;**105:**539–42.
26. Roy C, Slimani A, De Meester C, Amzulescu M, Pasquet A, Vancraeynest D *et al.* Age and sex corrected normal reference values of T1, T2 T2∗ and ECV in healthy subjects at 3 T CMR. *J Cardiovasc Magn Reson* 2017;**19**:72.
27. Bönner F, Janzarik N, Jacoby C, Spieker M, Schnackenburg B, Range F *et al.* Myocardial T2 mapping reveals age- and sex-related differences in volunteers. *J Cardiovasc Magn Reson* 2015;**17**:9.
28. Eghbali M, Eghbali M, Robinson TF, Seifter S, Blumenfeld OO. Collagen accumulation in heart ventricles as a function of growth and aging. *Cardiovasc Res* 1989;**23**:723–9.
29. Biernacka A, Frangogiannis NG. Aging and cardiac fibrosis. *Aging Dis* 2011;**2**:158–73.
30. Wassmuth R, Prothmann M, Utz W, Dieringer M, von Knobelsdorff-Brenkenhoff F, Greiser A *et al.* Variability and homogeneity of cardiovascular magnetic resonance myocardial T2-mapping in volunteers compared to patients with edema. *J Cardiovasc Magn Reson* 2013;**15**:27.
31. Von Knobelsdorff-Brenkenhoff F, Prothmann M, Dieringer MA, Wassmuth R, Greiser A, Schwenke C *et al.* Myocardial T1 and T2 mapping at 3 T: reference values, influencing factors and implications. *J Cardiovasc Magn Reson* 2013;**15**:53.